UNIVERSITY OF CALIFORNIA, IRVINE BRIDGE COLUMN TESTS

OVERVIEW:

The University of California, Irvine (UCI) has a research contract with CALTRANS to perform static, cyclic load tests on seismically retrofitted, reinforced-concrete bridge columns. This project is under the direction of Professor Gerry Pardoen at UCI (gpardoen@e4e.oac.uci.edu) and Mr. Tim Leahy (tleahy@trmx2.dot.ca.gov) at CALTRANS. The primary purpose of these tests is to study the relative strength and ductility provided by two retrofit construction procedures. The first procedure extends the diameter of the existing column with cast-in-place concrete. The second procedure extends the diameter of the existing column using shotcrete that is sprayed onto the exterior of the existing column. With funds obtained through Los Alamos National Laboratory's (LANL) University of California interaction office, staff from the LANL's Engineering Analysis Group and a faculty member from the Mechanical Engineering Department at Rose-Hulman Institute of Technology were able to perform experimental modal analyses on the columns. These modal tests were performed at various stages during the static load cycle testing. Results obtained from the experimental modal analyses provide further insight into the relative effectiveness of the two retrofit procedures.

In addition, data form these modal tests were analyzed with various parametric and non-parametric damage identification algorithms. From a damage identification standpoint one of the unique features of these tests was the ability to examine the effects of column pre-load on the damage identification process with varying amounts of damage input to the structure in a controlled and quantified manner. Also, the concrete column tests provided these investigators' with their first experience in applying damage identification algorithms to reinforced concrete structures.

The data from these tests are provided on this web site for others to analyze. Also, provided on this site are the ABAQUS input files for the accompanying finite element analyses. A description of the structures, the testing and results obtained is given below.

TEST STRUCTURE DESCRIPTION

The test structures consisted of two 24-in-dia (61-cm-dia) concrete bridge columns that were subsequently retrofitted to 36-in-dia (91-cm-dia) columns. The first column tested, labeled Column 3, was retrofitted by placing forms around existing column and placing additional concrete within the form. The second column, labeled Column 2, was extended to the 36-in-diameter by spraying concrete in a process referred to as shotcreting. The shotcreted column was then finished with a trowel to obtain the circular cross-section.

The 36-in-dia. portions of both columns were 136 in. (345 cm) in length. The columns were cast on top of 56-in-sq. (142-cm-sq.) concrete foundation that was 25-in-high (63.5-cm-high). A 24-in-sq. concrete block that had been cast integrally with the column extends 18-in. above the top of the 36-in-dia. portion of the column. This block was used

to attach the hydraulic actuator to the columns for static cyclic testing and to attach the electro-magnetic shaker used for the experimental modal analyses. As is typical of actual retrofits in the field, a 1.5-in-gap (3.8-cm-gap) was left between the top of the foundation and the bottom of retrofit jacket. Therefore, the longitudinal reinforcement in the retrofitted portion of the column did not extend into the foundation. The concrete foundation was bolted to the 2-ft-thick (0.61-m-thick) testing floor in the UCI laboratory during both the static cyclic tests and the experimental modal analyses. The structures were not moved once testing was initiated. Figure 1 shows the test structure geometry.

The columns were constructed by first placing the foundations on July 18th, 1997. Then the 24-in-diameter columns were placed on August 19th and the retrofits were added on September 19th. Corresponding portions of both test structures were constructed from the same batch of concrete. The only measured material property for these columns was the 28-day ultimate strength of the concrete and the test day ultimate strength. The 28-day ultimate strength of foundations was 4600 psi (32 MPa).   Test day ultimate strength was
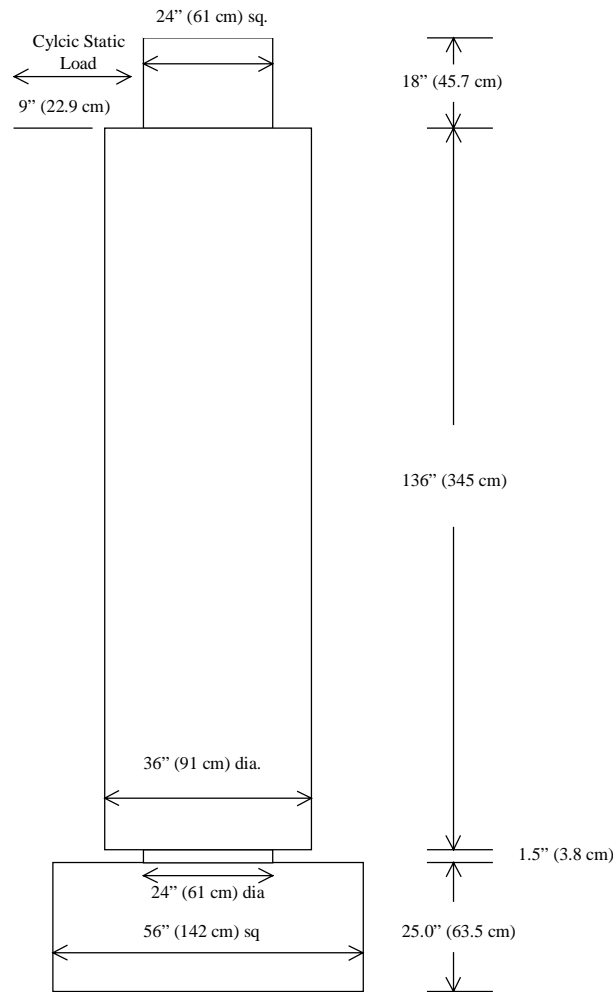

Fig. 1 Column Dimensions

not measured for the foundations. The 24-in-dia. column 28-day ultimate strength was 4300 psi (30 MPa) and the test day ultimate strength was 4800 psi (33 MPa). The 28-day-ultimate strength of the retrofit portion of the structures was 5200 psi (36 MPa). On test day the strength of the retrofit concrete was found to be 4900 psi (34 MPa).

Within the 24-in-dia initial column reinforcement consisted of an inner circle of 10 #6 (3/4-in-dia, 19-mm-dia) longitudinal rebars with a yield strength of 74.9 ksi (516 MPa). These bars were enclosed by a spiral cage of #2 (1/4-in-dia, 13.5-mm-dia) rebar having a yield strength of 30 ksi (207 MPa) and spaced at a 7-in pitch (18 cm). Two-inch-cover (5- cm-cover) was provided for the spiral reinforcement. The retrofit jacket had 16 #8 (1-in-dia, 25-mm-dia) longitudinal rebars with a yield strength of 60 ksi (414 MPa). These bars were enclosed by a spiral cage of #6 rebar spaced at a 6-in pitch (15 cm). The spiral steel also had a yield strength of 60 ksi. Again, 2-in.-cover was provided for this reinforcement. Lap-splices 17-in (43-cm) in length were used to connect the longitudinal reinforcement of the existing 24-in column to the foundation.

STATIC LOADING

Prior to applying lateral loads, an axial load of 90 kips (400 kN) was applied to simulate dead loads that an actual column would experience. A steel beam was placed on top of the column. Vertical steel rods, fastened to the laboratory floor, were tensioned by jacking against the steel beam that, in turn, applied a compressive load to the column. A photo of the test configuration is shown in Fig. 2.
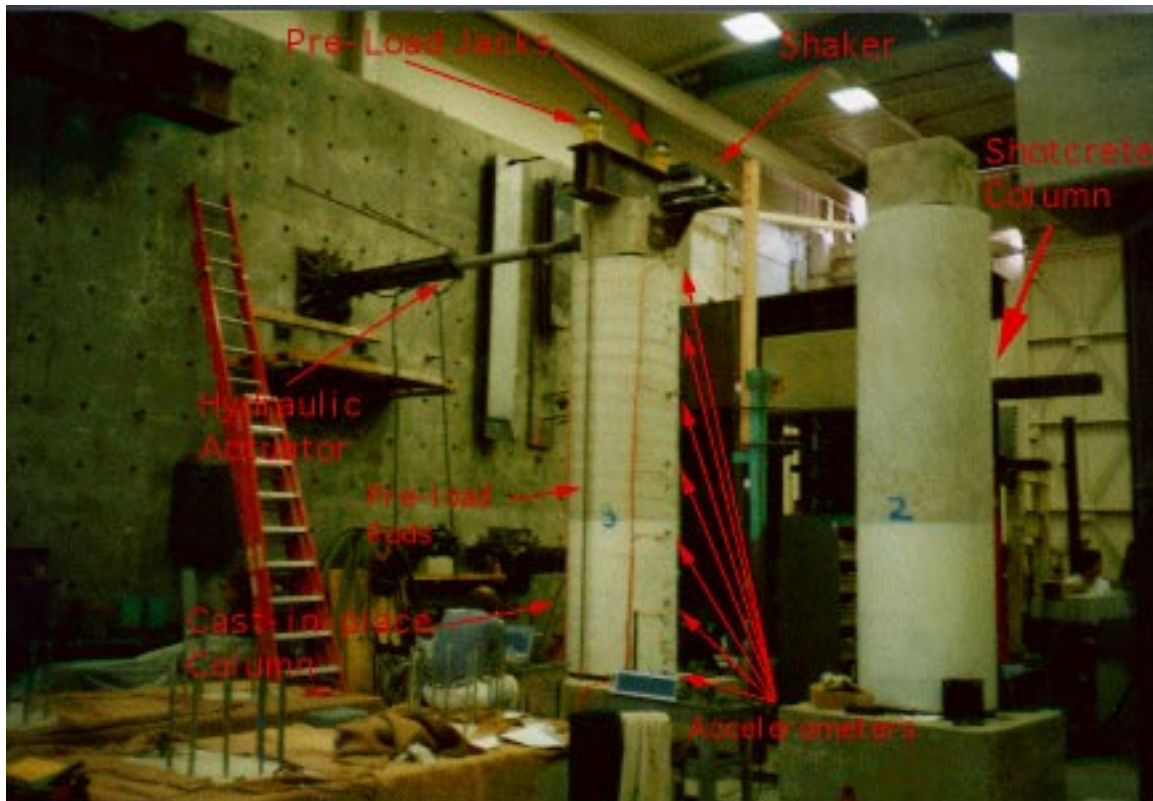

Fig. 2 Test Configuration.

An hydraulic actuator was used to apply lateral load to the top of the column in a cyclic manner. The loads were first applied in a force-controlled manner to produce lateral deformations at the top of the column corresponding to $0.25\Delta y_T$, $0.5\Delta y_T$, $0.75\Delta y_T$ and Δy_T. Here Δy_T is the lateral deformation at the top of the column corresponding to the theoretical first yield of the longitudinal reinforcement. The reader is referred to http:\\www.ics.uci.edu./~athomas/caltrans for a more detailed summary of the calculation of the deformation corresponding to first yield. The structure was cycled three times at each of these load levels.

Based on the observed response, a lateral deformation corresponding the actual first yield, Δy, was calculated and the structure was cycled three times in a displacement-controlled manner to that deformation level. Next, the loading was applied in a displacement-controlled manner, again in sets of three cycles, at displacements corresponding to $1.5\Delta y$, $2.0\Delta y$, $2.5\Delta y$, etc. until the ultimate capacity of the column was reached. Load deformation curves for columns 3 and 2 are shown in Figs 3 and 4, respectively. This manner of loading put incremental and quantifiable damage into the structures. The axial load was applied during all static tests.
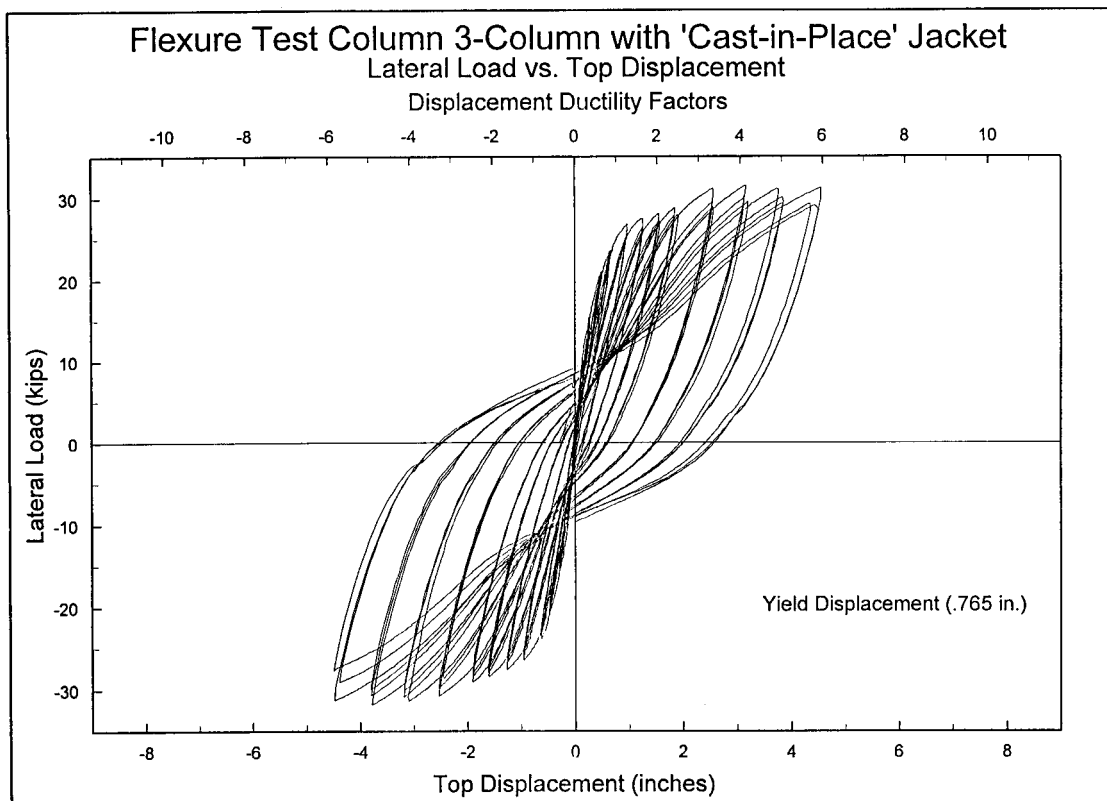

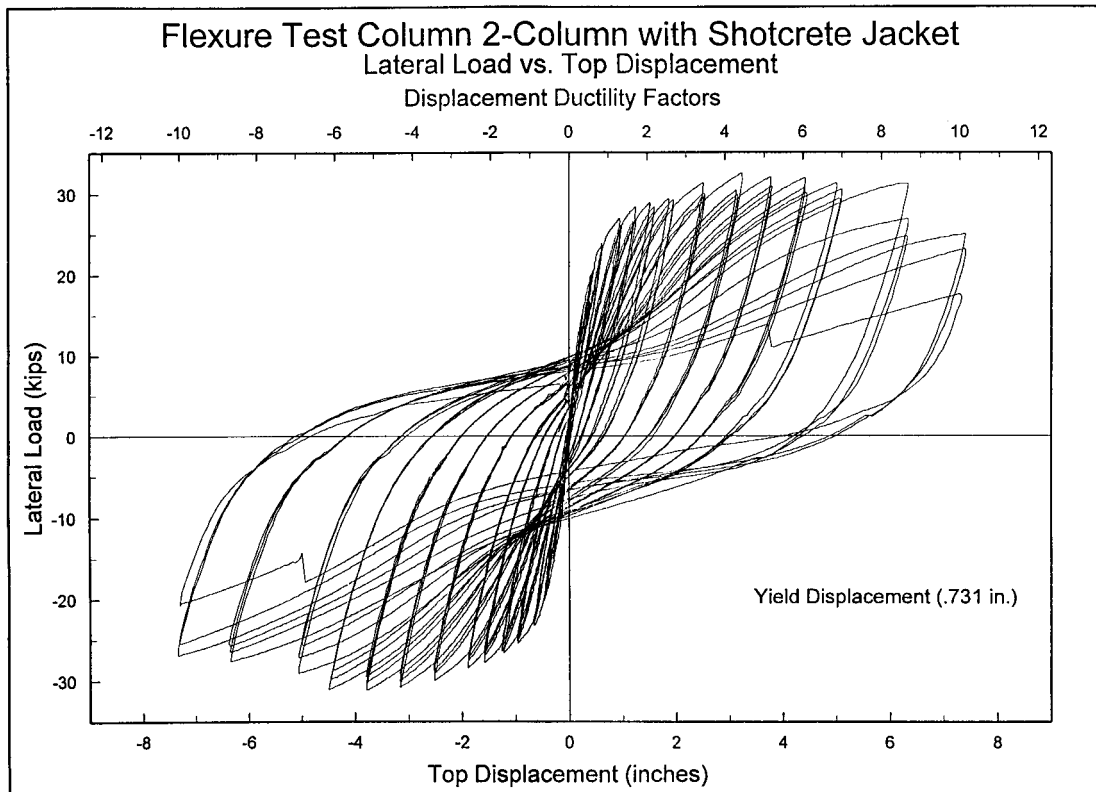Fig. 3 Load –displacement curves for the cast-in-place column.

Fig. 4 Load-displacement curves for the shotcrete column.

DYNAMIC EXCITATION

For the experimental modal analyses the excitation was provided by an APS electro-magnetic shaker mounted off-axis at the top of the structure. The shaker is shown in Fig 5. The shaker rested on a steel plate attached to the concrete column. Horizontal load was transferred from the shaker to the structure through a friction connection between the supports of the shaker and the steel plate. This force was measured with an accelerometer mounted to the sliding mass of the shaker 0.18 lb-s^2/in (31 Kg). A 0 - 400 Hz uniform random signal was sent from a source module in the data acquisition system to the shaker, but feedback from the column and the dynamics of the mounting plate produced an input signal that was uniform over the specified frequency range. Fig. 6 shows a typical input power spectrum. The same level of excitation was used in all tests except for one at twice this nominal level that was performed as a linearity check.

DATA ACQUISITION

Forty accelerometers were mounted on the structure as shown in Fig. 7. Note that locations 2, 39 and 40 had PCB 302A accelerometers. These accelerometers have a nominal sensitivity of 10mV/g and were not sensitive enough for the measurements being made. Locations 33, 34, 35, 36, and 37 were Wilcoxon 736t accelerometers that had a nominal sensitivity of 100mV/g. All other channels were PCB 336C accelerometers with
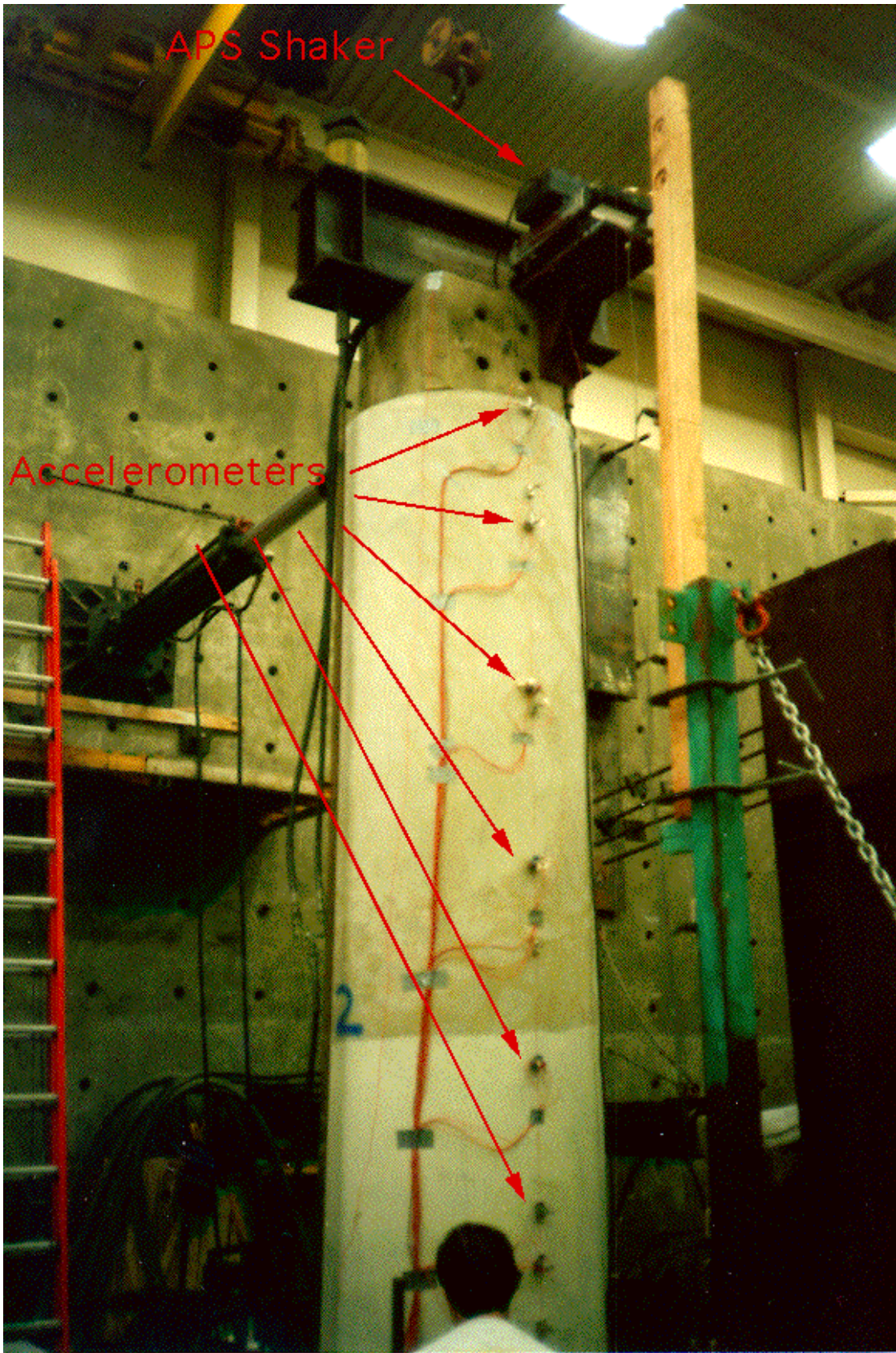
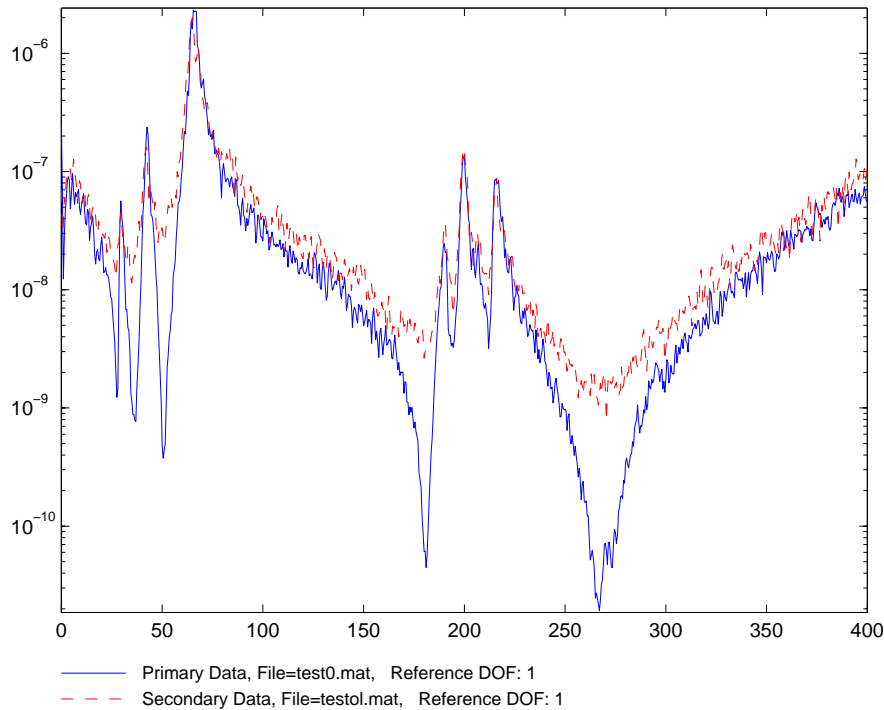Fig. 5 Shaker used during experimental modal analyses.

Fig. 6 Input Power Spectra.

a nominal sensitivity of 1V/g. During the test on the shotcrete column (column 2) the 336C accelerometer at location 23 had to be replaced with a PCB 308b02 accelerometer that had a sensitivity of 1V/g. All calibration factors were entered into the data acquisition system prior to the measurements. A calibration factor of 1.0 was entered for the accelerometer that monitored the sliding mass on the shaker.

Data was sampled and processed with a Hewlett-Packard (HP) 3566A dynamic data acquisition system. This system includes a model 35650 mainframe, 35653A source module used to drive the shaker, 5 35653A 8-channel input modules which provided power for accelerometers and performed the analog to digital conversion of accelerometer signals, and a 35651C signal processing module that performed the needed Fast Fourier Transform calculations. A Toshiba Tecra 700CT Laptop was used for data storage and as a platform for the HP software that controls the data acquisition system.

 Data acquisition parameters were specified such that frequency response functions (FRFs), input and response power spectra, cross-power spectra and coherence functions in the range of 0-400 Hz could be measured. Each spectrum was calculated from 30 averages of 2-s-long time-histories discretized with 2048 points. These sampling parameters produced a frequency resolution of 0.5 Hz. Hanning windows were applied to all measured time-histories prior to the calculation of spectral quantities.

A second set of measurements was acquired from 8-s-long time-histories discretized with 8192 points. Only one average was measured. A uniform window was specified for these data, as the intent was to measure a time history only.
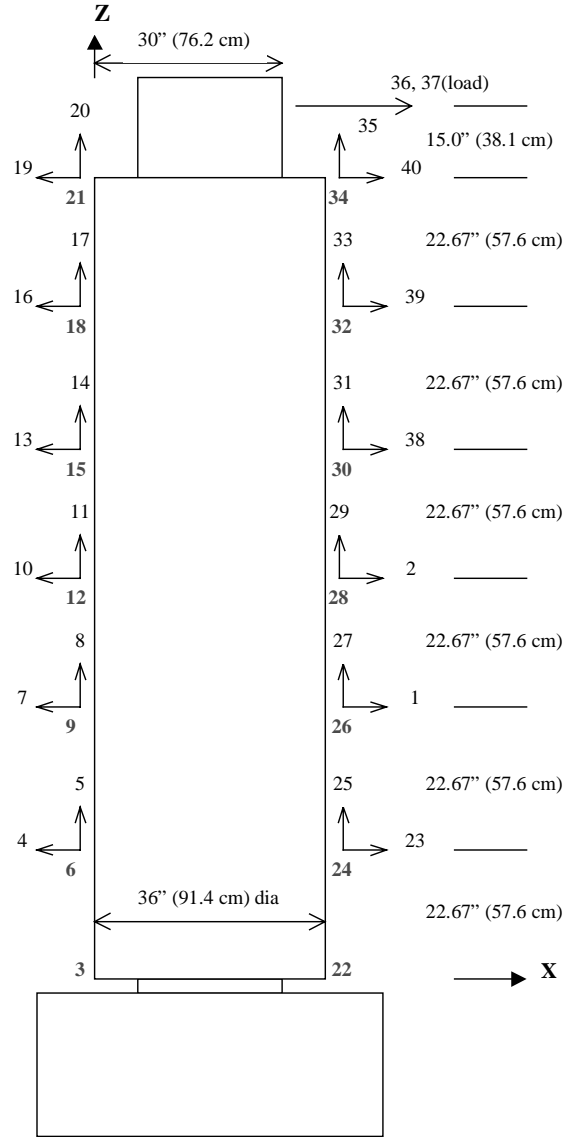

Fig. 7 Accelerometer locations and coordinate system for modal testing. Red numbers indicate accelerometers mounted in the –y direction. Accelerometers 1, 3 – 32 are PCB 336C with 1V/g sensitivity. Accelerometer 23 was replaced during test on the shotcreted column (Column 2) with a PCB 308b02 that had 1V/g sensitivity. Accelerometers 2, 39 and 40 are PCB 302A with 10mV/g sensitivity. Accelerometers 33-37 are Wilcoxon 736t with 100mV/g sensitivity. Accelerometers 36 and 37 are located 8 in (20. 3 cm) off axis in the –y direction.

DATA FILES

Data that was collected during the experimental modal analyses are described below. All files are in Universal File (Type 58) Format. In general, FRF and time-history measurements made at each damage level were done both with and without the pre-load applied.

Files are designated TEST#*
Where # indicates the sequential test number and * is a suffix indicating the type of test. The suffixes are:
P – indicate pre-load was applied
T-indicates time history measurement
L- test performed using twice the excitation level

Note that no "T" implies a test where FRFs based on 30 averages were measured. These files include the last time history used to form the average. No "P" indicates a test where the pre-load had been removed.

Undamaged Tests on Cast-In-Place Column 10/21/97
TEST0
TESTOT
TESTOL
TESTOP
TESTOPT
Tests on Cast-In-Place Column cycled to the theoretical first yield of the rebar, Δy 10/21/97
TEST1
TEST1T
TEST1P
TEST1PT
Tests on Cast-In-Place Column cycled to 1.5 Δy 10/21/97
TEST2T
TEST2P
TEST2PT
Tests on Cast-In-Place Column cycled to 2.5 Δy 10/21/97
TEST3
TEST3T
TEST3P
TEST3PT
Tests on Cast-In-Place Column cycled to 4.0 Δy 10/21/97
TEST4
TEST4T
TEST4P
TEST4OPT
Tests on Cast-In-Place Column cycled to 7.0 Δy 10/21/97
TEST5

TEST5T
TEST5P
TEST5PT
Undamaged Tests on Shotcrete Column 10/23/97
TEST6
TEST6T
TEST6P
TEST6PT
Tests on Shotcrete Column cycled to theoretical first yield of rebar, Δy 10/23/97
TEST7
TEST7T
TEST7P
TEST7PT
Tests on Shotcrete Column cycled to 1.5 Δy 10/23/97
TEST8
TEST8T
TEST8P
TEST8P
Tests on Shotcrete Column cycled to 2.5Δy 10/23/97
TEST9
TEST9T
TEST9P
TEST9PT
Tests on Shotcrete Column cycled to 4.0 Δy 10/23/97
TEST10
TEST10T
TEST10P
TEST10PT
Tests on Shotcrete Column cycled to 7.0 Δy10/23/97
TEST11
TEST11T
TEST11P
TEST1PT

FINITE ELEMENT ANALYSIS

Two finite element models were constructed so that results of analytical modal analyses can be compared to the experimental modal analysis results. This first model was constructed with 8-node continuum elements. This model had 20,979 degrees of freedom (DOFs). An elastic modulus of 3.6×10^6 psi (24.8 GPa$)$, a mass density of 2.17×10^{-4} lb-s^2/in^4 (2.28×10^3 kg/m^3), and a Poisson's ratio of 0.2 were specified in this model. The nodes corresponding to the base of the foundation were constrained in the three translation DOFs to simulated the connection to the structural testing floor. The mesh for this model is shown in Fig. 8. As shown in Fig. 8, the pre-load hardware was not modeled in any manner.

A similar model was analyzed with the pre-load simulated. To simulate the pre-load, a uniform pressure was applied vertically downward on the top surface of the 24-sq.-in. portion of the column. The deformed shape of the column was then used in a subsequent analytical modal analysis. This modeling does not account for the kinematic constraint provided by the pre-load hardware at the top of the column. As summarized in Table I, no significant difference was observed in the calculated resonant frequencies when the pre-load was applied in the manner described above .

A second model was constructed from three-node beam elements. This model had 114 DOFs. The same material properties specified in the continuum model were also used in this model. One beam element was used to model the foundation and one beam element was used to model the 1.5-in-deep section of the 24-in-dia. column. Fixed boundary conditions were applied to the base of the element that simulated the concrete foundation. For certain portions of this model, in particluar the foundation and the 1.5-in-high portion of the 24-in-dia. column, it is suspect if the beam elements can accurately model the behavior of the structure.

The results from the analytical modal analyses using both these models are summarized in Table I. Figures 9-11 show the first three bending modes, first two torsion modes and first axial mode calculated with the continuum element model and without pre-load. These are all modes that were calculated below 400 Hz. Note that because of symmetry, the bending modes occur in orthogonal pairs at the same natural frequency. The first three bending modes calculated with the beam models are shown in Fig. 12. Reinforcement was not incorporated in either model. Both ABAQUS input decks are made available in ASCII format. The continuum model is named UCI-Brick and the beam model is named UCI-Beam. Both models have nodes located in positions corresponding to the locations of the accelerometers and a pre-load applied.

TABLE I			
Finite Element Modal Analysis Results			
	Continuum Model Resonant Frequencies (Hz)	Continuum Model (with pre-load) Resonant Frequencies (Hz)	Beam Model Resonant Frequencies (Hz)
First Bending Mode	19.1	19.1	25.6
First Torsion Mode	114.	114.	131.
Second Bending Mode	124.	124.	136.
First Axial Mode	181.	181.	204.
Third Bending Mode	306.	306.	319.
Second torsion Mode	351.	351.	389.
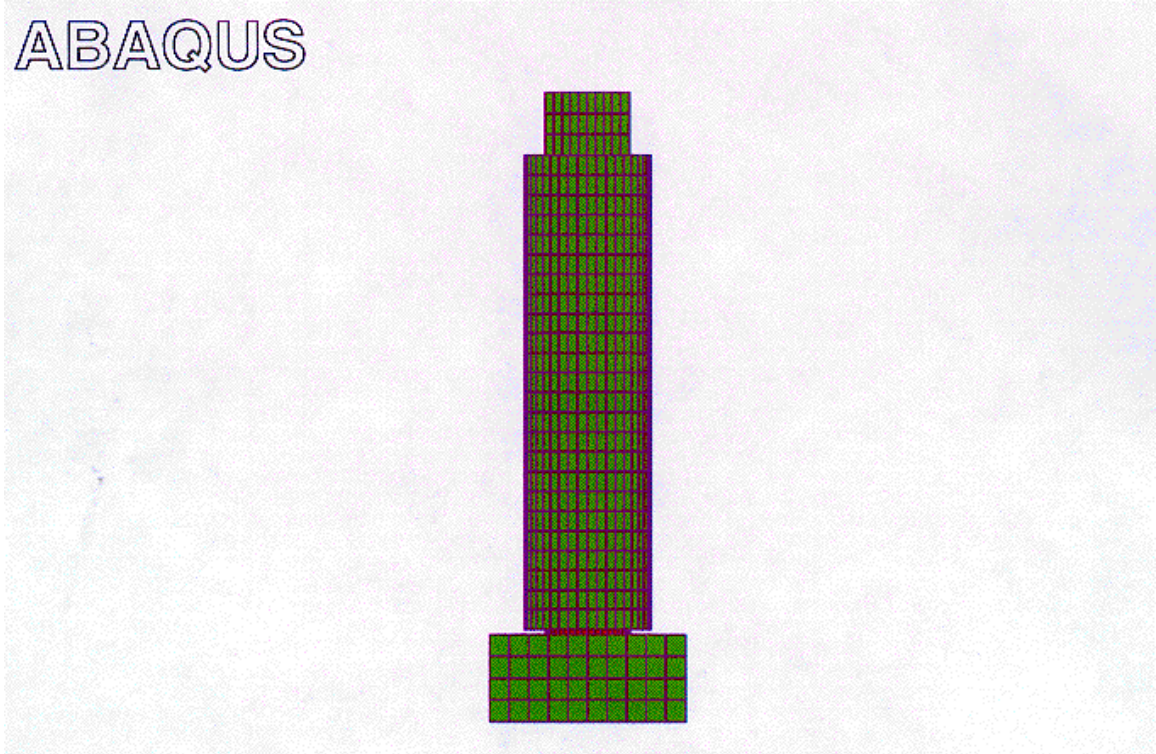
Fig. 8 Undeformed Mesh of the continuum model.
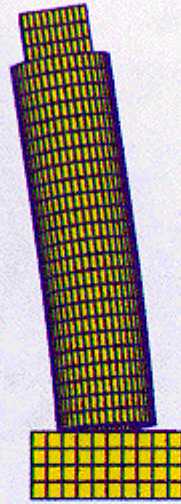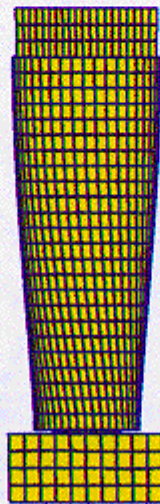
Fig. 9. (A) First bending mode and (B) first torsion mode calculated with the continuum model.
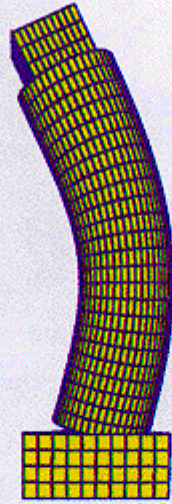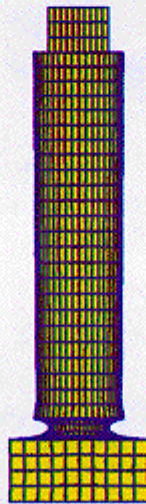
Fig. 10. (A) Second bending mode and (B) first axial mode calculated with the continuum model.
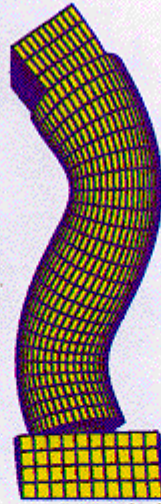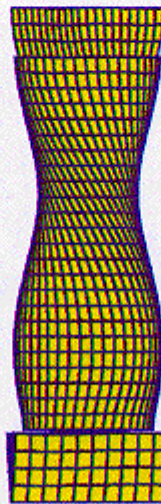
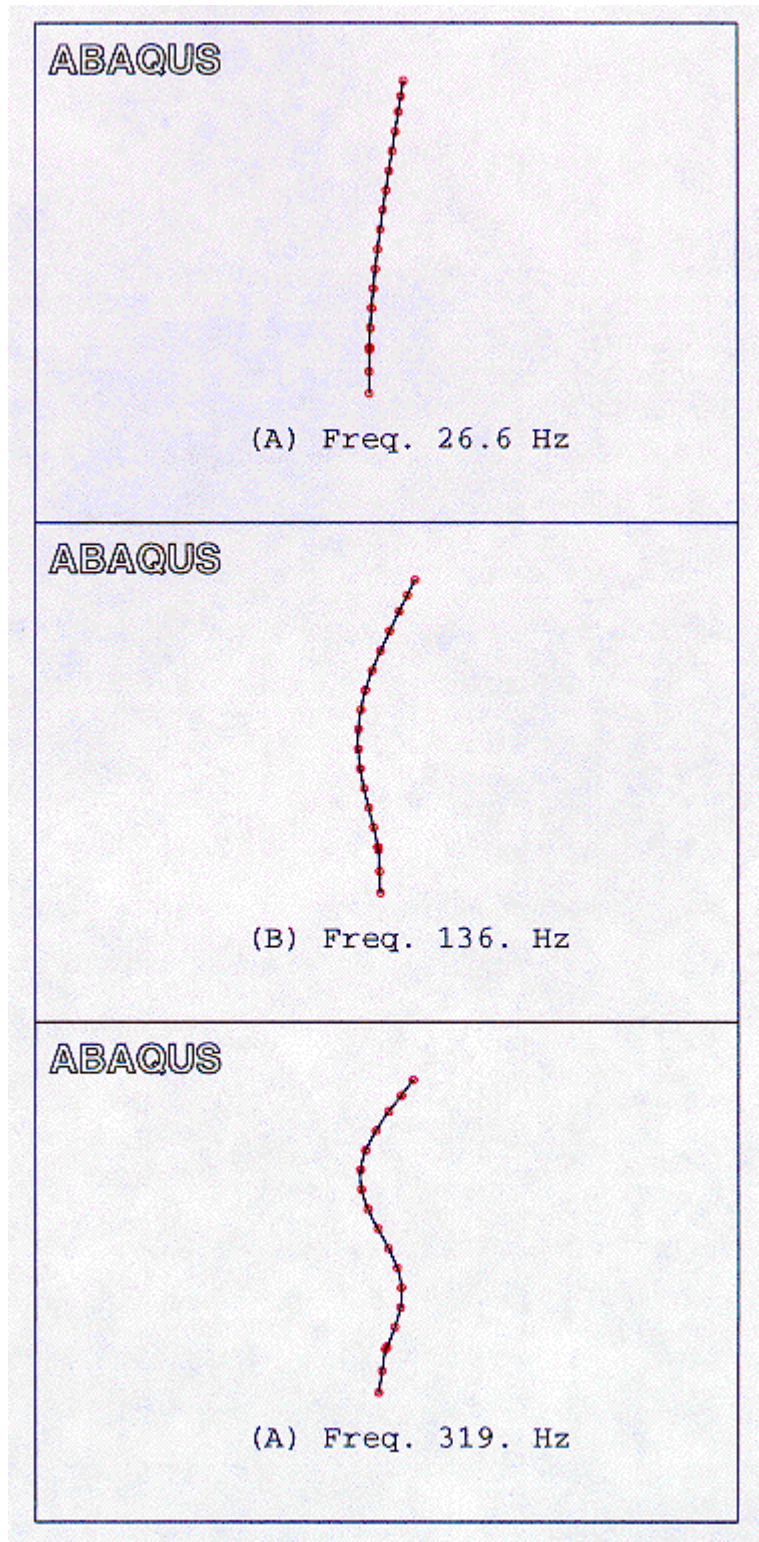Fig. 11. (A) Third bending mode and (B) second torsion mode calculated with the continuum model.

Fig. 12. (A) First bending mode, (B) second bending mode, and (C) third bending mode calculated with the beam model.

EXPERIMENTAL MODAL ANALYSIS RESULTS (TO COME)

DAMAGE DETECTION (TO COME)